Pergamon

Cement and Concrete Research 31 (2001) 1837–1845

CEMENT AND CONCRETE RESEARCH

Effect of speciation on the apparent diffusion coefficient in nonreactive porous systems

K.A. Snyder[a,*], J. Marchand[b]

[a]*Building Materials Division, National Institute of Standards and Technology, 100 Bureau Drive, MS 8621, Gaithersburg, MD 20899-8621, USA*
[b]*CRIB-Département de Génie Civil, Université Laval, Québec, Canada G1K 7P4*

Received 23 January 2001; accepted 10 September 2001

Abstract

A combined theoretical and experimental study of the effect that concentration and ionic speciation have on the apparent diffusion coefficient is performed using a nonreactive porous material in a divided cell diffusion apparatus. Varying the ionic species concentration over two orders of magnitude changes the apparent diffusion coefficient by no more than 20% for the systems studied. By contrast, at fixed ionic concentration, varying the ionic species changes the initial apparent diffusion coefficient by a factor of two. Over longer periods of time, the apparent diffusion coefficient varies in time, increasing by a factor of ten or more. For one system, the macroscopic diffusion potential across the specimen induces a transient *negative* apparent diffusion coefficient; iodide ions are transported from regions of low iodide concentration to regions of high iodide concentration. The theoretical analysis shows that, in nonreactive porous systems, the behavior of all the concentrations and species studied can be completely characterized by an electro-diffusion system of equations that contain two time-independent constants: the porosity and the formation factor. The relationship between these results and the prediction of concrete performance in the field is discussed. Published by Elsevier Science Inc.

Keywords: Pore solution; Diffusion; Electrochemical properties; Transport properties; Modeling

1. Introduction

There has been recent interest in the effect of ionic strength on the apparent diffusion coefficient in cementitious systems [1–5]. While a concentration-dependence has been observed, its relative impact on the apparent diffusion coefficient has not been compared directly to that of speciation (the particular ionic species present). Ushiyama and Goto [6] studied the effects of speciation on cement pastes, but no direct comparison was made to the effects of concentration. One possible reason for the lack of a direct comparison is the complexity and stability of cementitious systems and the relative difficulty of controlling the pore solution speciation.

Recently, a commercial alumina porous ceramic frit has been used as a model material for studying diffusive transport in nonreactive porous systems [7]. Its low surface charge makes this material an ideal candidate for a porous nonreactive substrate that can exhibit nearly ideal diffusive transport characteristics since surface effects and binding can be neglected. In addition, since the material is the result of a controlled industrial process, the diffusive transport properties are very consistent among replicate specimens.

Using the commercial frit as a model material, two series of experiments were performed. The first series used solutions of identical initial ionic species, with concentrations varying over two orders of magnitude. The second experimental series used identical initial ionic concentrations, but with varying counter-diffusing ionic species.

Similarly, numerical calculations were performed using the experimental parameters. The electro-diffusion equation [8] was used as a model for diffusive ionic transport that incorporates ion–ion interactions and accounts for the electrical diffusion potential that arises. The electro-diffusion transport equation was solved numerically and the estimated diffusion cell concentrations recorded for comparison to experimental data.

In the absence of chemical reaction, the transport equation characterizing ionic diffusion in concentrated electrolytes requires only two time-independent parameters: the

* Corresponding author. Tel.: +1-301-975-4260; fax: +1-301-990-6891.
E-mail address: kenneth.snyder@nist.gov (K.A. Snyder).

0008-8846/01/$ – see front matter Published by Elsevier Science Inc.
PII: S0008-8846(01)00679-2

porosity and the formation factor. The electro-diffusion equation and these two parameters are shown to be sufficient to characterize the time-dependent behavior of the experimental systems, including a time-dependent apparent diffusion coefficient. Moreover, the transport equation was capable of predicting the occurrence of a transient *negative* apparent diffusion coefficient for one of the systems.

The fact that the apparent diffusion coefficient can vary in time in nonreactive systems raises important questions regarding the validity of using a linear Fickian transport equation with an apparent diffusion coefficient to characterize the service life of a cementitious system. In contrast, a properly formulated transport equation based on the electro-diffusion equation, along with the porosity and the formation factor, can fully characterize the time-dependent behavior of multispecies transport in these nonreactive systems.

Studying nonreactive systems is a meaningful way to verify current understanding of diffusive transport. The pore solution of cementitious systems is composed of a concentrated electrolyte containing a diverse population of ionic species. Service life models that attempt to simulate behavior must rely heavily on their prediction of ionic transport within the structure [9–11]. In order to have confidence in the performance of a transport model of a cementitious system, one must first be confident of the transport model's performance in an idealized system.

Validation of a diffusive transport model for cementitious systems containing concentrated electrolytes is vital to a service life model that also incorporates chemical reaction. Precipitation and dissolution of minerals present within the microstructure can have dramatic effects on the transport coefficients. Accurate estimates of the extent of a reaction can only be achieved with accurate estimates of the activity of each species present [12,13]. Further, accurate models of binding and chemical reaction require not only the ionic activity, but must also consider the time-dependent competition among transport, binding and reaction [14]. Without detailed knowledge of diffusive transport, models for dependent processes such as chemical reaction and binding become suspect since they depend on accurate estimates of the species activity.

2. Coupled diffusive transport

Historically, ionic transport in cementitious systems has been characterized by Fick's law of diffusive transport [9]. The flux $\mathbf{j}_i$ of the i-th ionic species is proportional to the gradient in the amount-of-substance concentration c_i of that species, with the proportionality being the apparent diffusion coefficient D_i^{a} of that species [15]:

$$\mathbf{j}_i = -D_i^{\mathrm{a}} \nabla c_i \tag{1}$$

(Vector quantities are denoted in bold-type face.) For concentrated electrolytes, this equation quickly becomes inadequate due to ion–ion interactions. One method to address this is to use a tensor diffusion coefficient [16] so that ion–ion effects are incorporated in an empirical manner. Unfortunately, this requires extensive experimental data before one can apply this approach.

An alternative approach is to incorporate the ion–ion interactions at a fundamental level so that one directly calculates the effects of having other species present. Fortunately, this can be achieved in a relatively straightforward manner. The electro-diffusion equation as a model for the transport of ionic species has been used in solid-state systems [8], biological systems [17,18] and cementitious systems [4,5,19–22]. While it has been used to successfully characterize observed transport in cement and concrete systems, it is also useful for systematic studies of transport in nonreactive porous systems. As such, it is a powerful investigative tool for answering "what if" questions. Here, a systematic test of its applicability to porous systems is undertaken.

The electro-diffusion equation is formulated first for a bulk electrolyte. From this equation, the equation for a porous material is formulated using the principles of volume averaging over a representative elemental volume (REV) [23].

2.1. Flux equation

The electro-diffusion equation for an electrolyte, referred to elsewhere as the extended Nernst–Planck equation [19,20,24], is a transport equation that characterizes flux due to a gradient in the total chemical potential that is composed of the internal chemical potential and the external chemical potential due to an electrical potential [25]. Within the electrolyte, the flux $\mathbf{j}_i$ of the i-th species is proportional to the gradient in the internal chemical potential μ_i (molar basis) and the gradient in the diffusive electrical potential ψ_{D} (electrochemical potential) [26]:

$$\mathbf{j}_i = \frac{-D_i}{RT} c_i \nabla(\mu_i + z_i \mathcal{F} \psi_{\mathrm{D}}) \tag{2}$$

The quantity D_i is the diffusion coefficient within the electrolyte, z_i is the ionic valence, $\mathcal{F}$ is the Faraday constant, c_i is the ionic amount-of-substance concentration, R is the gas constant and T is the absolute temperature. The diffusion potential ψ_{D} arises due to variations in the self-diffusion coefficients of the various ionic species. The flux relationship in Eq. (2) has implicitly incorporated the Einstein relation between the diffusion coefficient D_i and the conventional ionic mobility u_i [26] (Eq. (3)):

$$D_i = RT\, u_i \tag{3}$$

Although this relationship is not exact for increasing ionic strengths, it is sufficiently accurate to capture the salient

behavior of experimental systems, as will be demonstrated subsequently.

The flux in Eq. (2) can be expressed in experimentally measurable variables by converting from chemical potential μ_i to chemical activity a_i, which can then be related to concentration through the mathematical construction of the activity coefficient γ_i [27] (Eq. (4)):

$$a_i = \gamma_i c_i \tag{4}$$

Making these substitutions leads to the electro-diffusive flux equation that is similar in form to those that have appeared elsewhere [4,7,19,20]:

$$\mathbf{j}_i = -D_i\left(1 + \frac{\partial \ln \gamma_i}{\partial \ln c_i}\right)\nabla c_i - \frac{\mathcal{F}}{RT} z_i c_i D_i \nabla \psi_D \tag{5}$$

The activity coefficients can be calculated using the Pitzer equations [28] and the method can be incorporated into a computer code such as was done for the PHRQPITZ program [29]. The above flux equation, in conjunction with the diffusion potential ψ_D, is sufficient to describe transport in nonreactive porous systems with negligible binding.

For this study, the diffusion potential was chosen in such a manner as to ensure that the electrolytic solution remains neutral; there is no excess charge. This is accomplished by enforcing zero total current $\boldsymbol{I}_T$ everywhere (nil current condition) [7]:

$$\boldsymbol{I}_T = \mathcal{F}\sum_i z_i \mathbf{j}_i = 0 \tag{6}$$

If the system is initially neutral ($\sum z_i c_i = 0$), the nil current condition will ensure electro-neutrality [8,24]. This approach is sufficient for diffusing species. An alternative approach is to solve the Nernst–Planck–Poisson system of equations [17,19,20].

2.2. Bulk equation

The previous system of equations, Eqs. (5) and (6), apply only to the electrolyte within the pores. For porous materials, one must be explicit whether the flux equation is for the pore space or for the pore space and solid structure combined (bulk). In this study, a bulk formulation is used. For the electro-diffusive flux in Eq. (5), it has been shown previously that the diffusion coefficient D_i that appears in Eq. (5) is the bulk *microstructural* diffusion coefficient ($D_i^{\mu} = D_i$), and is independent of the pore solution composition [7]; interactions within the pore solution are accounted for in the remaining terms in the equation. For a porous material with a formation factor F, the bulk microstructural diffusion coefficient appearing in Eq. (5) is proportional to the self-diffusion coefficient D^s [7]:

$$D_i^{\mu} = \frac{D_i^s}{F} \tag{7}$$

The self-diffusion coefficient of an ionic species is its diffusion coefficient in water in the limit of infinite dilution [30]. Eq. (7) reflects the fact that the bulk microstructural diffusion coefficient D_i^{μ} depends on the species i. It is important to realize that D_i^{μ} is not the apparent Fickian diffusion coefficient D_i^a. Rather, it simply characterizes the diffusion of an ionic species in the absence of electrostatic interactions.

Use of the formation factor originated in geological research and has been defined as the ratio of the conductivity of a pore solution σ_p to the bulk conductivity σ_b of a insulating porous material filled with that pore solution [31]:

$$F = \frac{\sigma_p}{\sigma_b} \tag{8}$$

In principle, the formation factor is a constant, at constant porosity and tortuosity (absence of chemical reaction with solid microstructure), for a particular porous material, and is independent of ionic species [7]. Since the self-diffusion coefficient of an ionic species is also a constant (at constant temperature), the flux equation for the N species has been reduced from a system of N equations with N apparent diffusion coefficients, as shown in Eq. (5), to a system of N equations with only a single parameter, the formation factor.

In practice, determining the formation factor must be performed with some care. In porous systems containing sufficient surface charge, the ratio of the pore solution conductivity to the bulk conductivity will depend on the pore solution concentration [32,33]. This concentration dependence is due to a surface conduction contribution to the measured conductivity [34,35]. In principle, this effect can be isolated, yielding the true microstructural formation factor that is required in the equations used here.

2.3. Time-dependent equation

The time-dependent behavior of the electro-diffusive system can be derived from conservation of mass. For a porous system with constant porosity ϕ, the rate change in concentration is proportional to the negative divergence of the bulk flux $\mathbf{j}_i^b$:

$$\phi\frac{\partial c_i}{\partial t} = -\nabla\cdot\mathbf{j}_i^b$$

$$= \frac{D_i^s}{F}\nabla\cdot\left(1 + \frac{\partial \ln \gamma_i}{\partial \ln c_i}\right)\nabla c_i + \frac{\mathcal{F}}{RT} z_i \frac{D_i^s}{F}\nabla\cdot c_i \nabla \psi_D \tag{9}$$

This time-dependent equation and Eq. (6) form a system of equations containing two variables (c and ψ_D) and two parameters (ϕ and F). Since the variables γ_i and ψ_D can be calculated from the physicochemical properties of the electrolyte, the two parameters ϕ and F completely

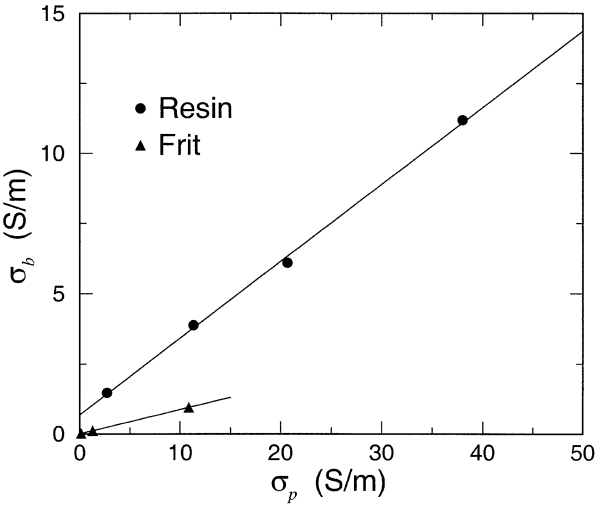

Fig. 1. The pore solution conductivity σ_p and the corresponding bulk conductivity σ_b for the resin system of McDuff and Ellis [38] and the frit systems used here.

characterize the time-dependent behavior of systems with arbitrary speciation.

Characterizing the electro-diffusion transport by Eqs. (9) and (6), which have the porosity and the formation factor as the only adjustable parameters, has great experimental advantages. The porosity of a cementitious material can be determined by a number of methods such as standardized test methods or mercury intrusion porosimetry. The formation factor can be determined from conductivity measurements [36] and pore extraction [37]. Therefore, it is conceivable that one could use appropriate transport equations to accurately predict the diffusive transport in a cementitious system without performing any diffusion measurements.

3. Porous frit

The diffusion experiments were performed on a commercial porous frit composed of a sintered alumina ceramic (99.8% alumina) measuring (50.76 ± 0.04) mm in diameter and (6.48 ± 0.03) mm thick; the uncertainty is an estimated standard deviation calculated from seven frits. The porosity, estimated from mercury intrusion porosimetry analysis, was approximately 0.26. The pore size distribution was concentrated between 350 and 450 nm, consistent with the manufacturer's intended use and published specification of a pore size less than 500 nm.

The alumina frit was regarded as a nearly ideal porous medium for studying diffusive transport. The alumina is chemically stable when in contact with solutions having a pH near 7. In addition, conductivity measurements suggest that the frit has a relatively low surface charge. As defined in Eq. (8), the formation factor F is calculated from the ratio of the pore fluid electrical conductivity σ_p to the bulk electrical conductivity σ_b with that pore fluid. The calculation can be repeated for different pore solutions with varying values of σ_p.

Such an experiment was performed in 1979 by McDuff and Ellis [38] on a model porous material composed of a packed column of cation exchange resin. Their raw data for large pore solution conductivities are denoted in Fig. 1 as filled circles. Linear ordinary least squares regression applied to the data reveal a positive intercept of (0.68 ± 0.17) S/m; the uncertainty is an estimated standard deviation. Similarly, one of the frits was saturated with

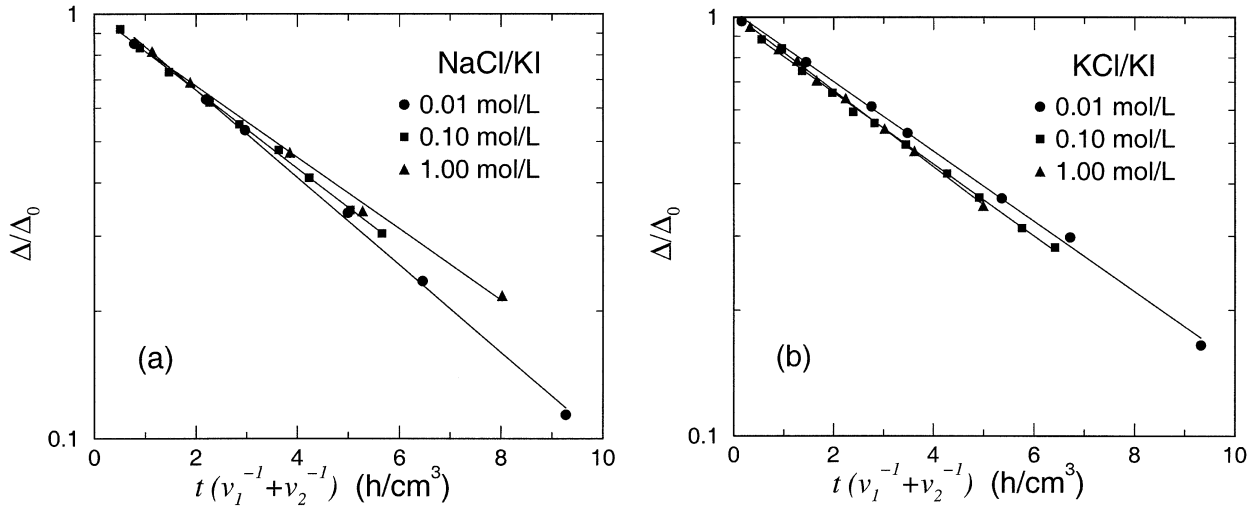

Fig. 2. Concentration difference Δ of iodide (filled symbols) for the (a) NaCl/KI and the (b) KCl/KI systems; the time t is scaled by the vessel volumes v_1 and v_2. The lines shown are the result of the linear regression analyses reported in Table 1. The measurement uncertainties were approximately the size of the symbols used.

different standard potassium chloride conductivity solutions [39], and the data are shown in Fig. 1 as filled triangles. For the frit, the intercept was only (0.00258 ± 0.00025) S/m. Since the intercept is proportional to the surface charge of the material [40], one expects that the surface charge of the frit is a factor of 263 times smaller than that of the resin. Although this does not imply that the surface charge on the frits is negligible, the data presented herein will show that an analysis that neglects binding still captures all the salient features of the effect speciation has on the diffusive transport of ions through these ceramic frits.

4. Experiment

The divided cell arrangement was used as the experimental apparatus because of its procedural simplicity. Since the ceramic specimens have a relatively large diffusion coefficient with respect to hydrated cement paste, usable data could be collected within a reasonable period of time. As mentioned previously, the ceramic material had a relatively small surface charge, surface adsorption effects could be neglected. The result is a material that should exhibit nearly ideal diffusive transport properties.

Iodide was chosen as the measured ionic species because commercial solid-state ion selective combination electrodes for iodide have experimental advantages over chloride electrodes. For each measurement, the electrode was standardized using reference iodide solutions.

Each ceramic frit was first mounted, using epoxy, into an acrylic annulus. After the epoxy had cured, the sample was saturated with a potassium iodide (KI) solution. The saturated frit was then clamped between two glass vessels, each having a capacity of approximately 250 mL, using rubber o-rings to make a water tight seal. One vessel was then filled with the same KI solution and the other vessel was filled with a test electrolyte. Both vessels were sealed to reduce evaporation, and then placed inside a walk-in environmental chamber maintained at 25 °C. All sampling and concentration measurements were performed within the chamber in order to ensure stability in both the diffusion and the measurements; there is a nominal 2 %/°C variation in the self-diffusion coefficient as a function of temperature [30], and the concentration measurement precision improved within the stable environment. Additional details of the experimental procedure are given elsewhere [7].

Table 1
Absolute value of the slopes calculated from the data for the NaCl/KI and the KCl/KI systems in Fig. 2, regressed to a linear model

Species	Concentration (mol/L)	|Slope| (cm^3/h)
NaCl/KI	0.010/0.010	0.2365 ± 0.0051
	0.100/0.100	0.2120 ± 0.0024
	1.024/1.000	0.1931 ± 0.0059
KCl/KI	0.010/0.010	0.1923 ± 0.0039
	0.100/0.100	0.1978 ± 0.0029
	1.000/1.000	0.2101 ± 0.0024

The uncertainties shown are the estimated standard deviations reported by the regression software, with a corresponding coverage factor of $k = 1$.

5. Analysis

The analysis of the experimental diffusion data is based on the "constant gradient" assumption [7]. For relatively large vessel volumes and a relatively thin specimen, the concentration profile across the specimen, after a suitable initialization time, is nearly a straight line. Based on this assumption, the concentration gradient across the sample is a constant, equal to the difference between cell concentrations, divided by the sample thickness L. Under these ideal conditions, Fick's law (Eq. (1)) should apply. For vessel volumes v_1 and v_2 and sample area A, the difference in concentration Δ between the two vessels can be shown to decay exponentially [7,41]:

$$\frac{\Delta}{\Delta_0} = exp\left[\frac{-D^a A}{L}\left(v_1^{-1} + v_2^{-1}\right)\, t\right] \tag{10}$$

The quantity Δ_0 is the concentration difference at the onset of a linear concentration profile. Based on Eq. (10), a semi-log plot of the concentration difference between the two vessels should appear as a straight line under ideal conditions; the magnitude of the slope being proportional to the apparent diffusion coefficient D^a. Deviations from a straight line will indicate behavior that cannot be modeled by Fick's law with a constant apparent diffusion coefficient.

6. Results

The results are separated for the two series of experiments. In the first series, the ionic species present were kept constant and the initial iodide concentration differences were varied. In the second, the initial iodide concentration was held constant, and the other species present were varied.

6.1. Varying concentration

The experiments with varying concentration were performed with either potassium chloride or sodium chloride as the counter-diffusing electrolyte. Plots of the experimental results are shown in Fig. 2. For both the KCl/KI and the NaCl/KI systems, the data exhibit virtually linear behavior on the semi-logarithmic axes. The apparent linear behavior suggests that these systems behave in a nearly "ideal" manner, and can be characterized accurately by Fick's law in Eq. (1). This ideal behavior is caused by the nearly equal self-diffusion coefficients for potassium, chloride and iodide. The corresponding electrical diffusion potential across the sample is relatively small.

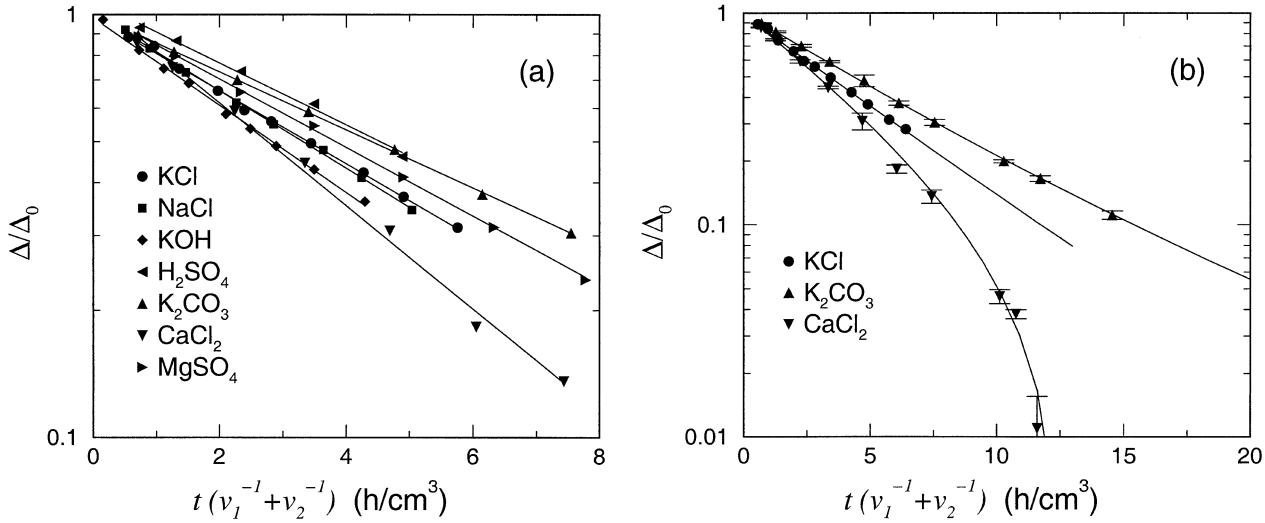

Fig. 3. Concentration difference Δ of iodide (filled symbols) as a function of scaled time. In (a), results from linear regression (solid lines) for $t(v_1^{-1}+v_2^{-1})<8$ h/cm^3; the calculated slopes are reported in Table 2. In (b), the electro-diffusion equation (solid lines) is used to estimate the formation factor F at long times; the calculated values of F are shown in Table 2. The error bars represent an estimated standard deviation.

The magnitude of the slope calculated from the data at each concentration is reported in Table 1. The uncertainties reported are the estimated standard deviations reported by the regression software, and have the corresponding coverage factor [42] $k=1$. The slopes for the NaCl/KI systems decreased by 18% as the iodide concentration increased. The slopes of the KCl/KI systems *increased* by 9% as the iodide concentration increased. Therefore, it is possible to observe both decreases and increases in the apparent diffusion coefficient as the concentration increases.

While the differences among slopes, being greater than the estimated uncertainties, suggest that the concentration dependence is statistically significant, for practical use, these variations are minor. Any chemical reactions that might occur within the cementitious matrix can alter the diffusion coefficient, easily overwhelming a 20% variation in the apparent diffusion coefficient due to variations in the concentration.

Table 2
Magnitude of the slope for data shown in Fig. 3a, regressed to a linear model for $t(v_1^{-1}+v_2^{-1})<8$ h/cm^3

Counter solution	Concentration (mol/l)	|Slope| (cm^3/h)	F
K_2CO_3	0.0769	0.1581 ± 0.0014	11.7
H_2SO_4	0.0859	0.1688 ± 0.0075	9.6
$MgSO_4$	0.1660	0.1867 ± 0.0022	13.5
KCl	0.1000	0.1978 ± 0.0029	11.4
NaCl	0.1000	0.2120 ± 0.0024	11.8
KOH	0.0879	0.2333 ± 0.0034	11.2
$CaCl_2$	0.0731	0.2801 ± 0.0089	12.8

For each system, the KI concentration was 0.10 mol/l. Also shown are the values for the formation factor F used to produce the solid curves Fig. 3b. The uncertainties shown are the estimated from standard deviations reported by the regression software, with a corresponding coverage factor of $k=1$.

6.2. Varying speciation

The experiments with varying speciation were performed with KCl, NaCl, KOH, K_2CO_3, $CaCl_2$, H_2SO_4 and $MgSO_4$ as the counter-diffusing electrolyte. In all cases, the initial concentration of KI was 0.10 mol/L. The concentration of each counter-diffusing electrolyte was varied to eliminate the osmotic pressure gradient across the ceramic specimen; it is not asserted that the values used here were ideal.

The relative concentration differences Δ/Δ_0 are shown in Fig. 3, and the analyses of the data are divided between the "short" time and the "long" time results. In Fig. 3a, a linear model is regressed to the data for which $t(v_1^{-1}+v_2^{-1})<8$ h/cm^3. The results from the linear regression analyses are shown in Table 2, and the corresponding lines are shown in Fig. 3a. The uncertainties reported are the estimated standard deviations reported by the regression software, and have the corresponding coverage factor [42] $k=1$. Based on these results, the $CaCl_2$/KI system and the K_2CO_3/KI system represent the extrema, and are shown in Fig. 3b over a longer time, along with the KCl/KI system as an example of nearly ideal behavior.

The results from the linear regression given in Table 2 give an indication of the effect speciation can have on the observed diffusion coefficient. The magnitude of the slopes shown in the table varies by nearly a factor of two. This contrasts the previous 20% change in the slopes due to changes in concentration.

7. Discussion

The data for each system were analyzed using Eq. (9). The porosity was fixed at 0.26 and the formation factor was the only remaining free parameter. The value of the forma-

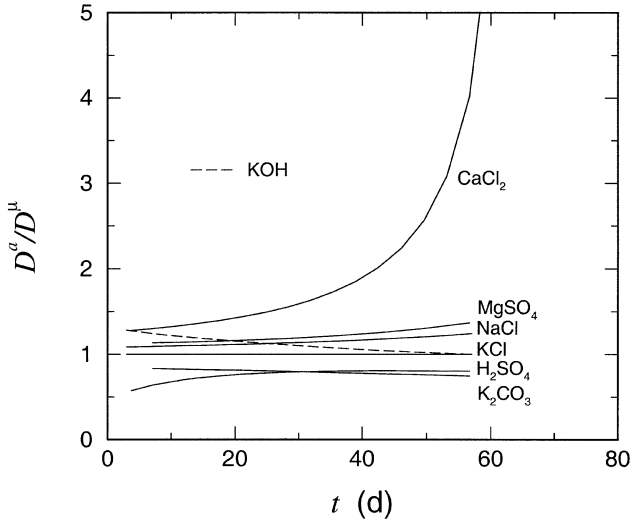

Fig. 4. The ratio of the apparent diffusion coefficient D^a to the microstructural diffusion coefficient D^{μ} (Eq. (7)) of iodide for the various counter diffusing electrolytes, as a function of time t.

tion factor F required to best approximate the experimental data is shown in Table 2 for each system. The coefficient of variation for these values was approximately 10%. The corresponding results are shown as solid curves in Fig. 3b. The curves for the other systems are not shown for clarity. Moreover, remaining systems had only minor curvature by comparison.

The $CaCl_2$ and the K_2CO_3 data are shown in Fig. 3b to delineate the envelope over which the concentrations could vary over long times. Note that the slope of each curve is not a constant. While the change in slope for the K_2CO_3/KI system is gradual, the change in slope for the $CaCl_2$/KI system is dramatic. Therefore, characterizing the iodide transport in the $CaCl_2$/KI system using Fick's law and a constant apparent diffusion coefficient is unwarranted. Further, the apparent iodide diffusion coefficient decreases in the K_2CO_3/KI system and increases in the $CaCl_2$/KI system. Any "adjustments" to an apparent diffusion coefficient to account for one system would certainly not be applicable to another. This is analogous to determining the apparent diffusion coefficient under one set of experimental conditions and using that to predict the behavior of the concrete in the field under a different species exposure.

The electro-diffusion equation can be used to quantify the magnitude of the nonideal behavior within each system. The apparent diffusion coefficient can be calculated at any time by using the slope of the curve calculated from the electro-diffusion equation. The calculated time-dependent apparent diffusion coefficient D^a can then be compared to the constant microstructural diffusion coefficient D^{μ}. The ratio of these two coefficients is shown in Fig. 4 for all of the systems.

The curves shown in Fig. 4 express quantitatively the deficiency in characterizing multispecies diffusion with a single apparent diffusion coefficient. Accurately characterizing the diffusive transport of iodide in these nonreactive systems using Fick's law requires an apparent diffusion coefficient that must vary in time. For the $CaCl_2$/KI system, the apparent diffusion coefficient increases by a factor of 5 at 60 days.

The behavior of the $CaCl_2$/KI system at very long time was very interesting. The curve for the $CaCl_2$/KI system in Fig. 3b appears to be diverging at long times. Analyzing the experiment using the electro-diffusion equation, one expects that the concentration difference between the vessels will eventually become *negative*. The measured concentration differences Δ for the $CaCl_2$/KI system beyond 60 days are shown in Fig. 5a on a linear scale. After approximately

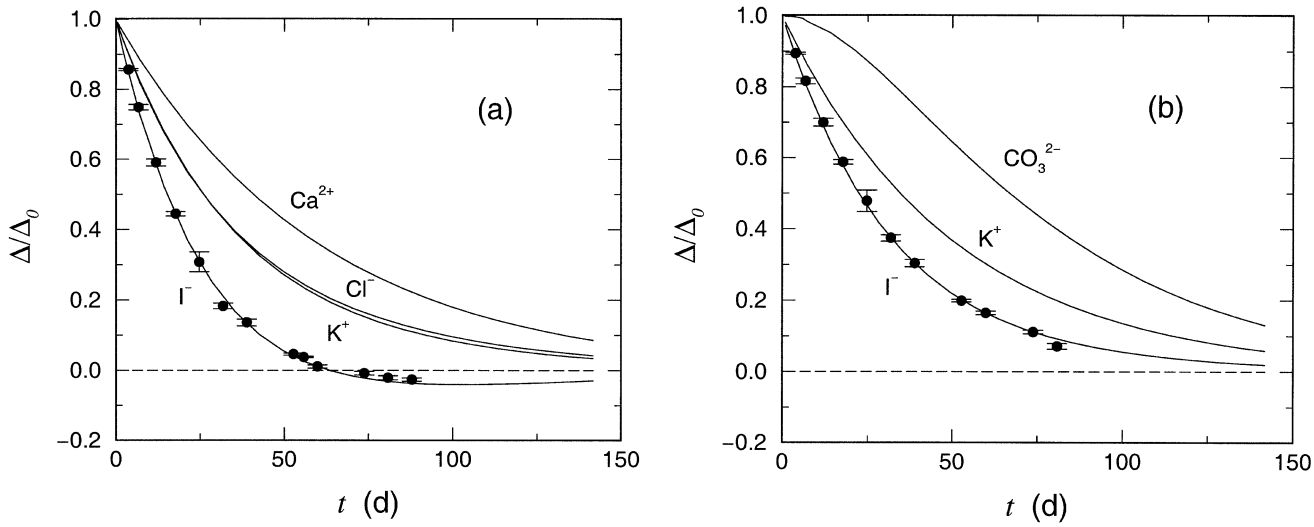

Fig. 5. Concentration difference Δ of each diffusing species in the (a) $CaCl_2$/KI and the (b) K_2CO_3/KI systems, each as a function of time t. The error bars represent an estimated standard deviation.

70 days, the observed concentration difference was, in fact, negative. As a means of comparison, the corresponding data for the K_2CO_3/KI system are shown in Fig. 5b.

A negative concentration difference Δ is significant. Based on Eq. (1), when the concentration difference Δ becomes negative, the concentration gradient ∇c changes sign. Since the experimentally measured flux is still pointing in the same direction, Eq. (1) is satisfied only by having a *negative* apparent diffusion coefficient D^a. Similarly, based on Eq. (1), the only way to diffuse a species from regions of low concentration to regions of higher concentration is through a negative diffusion coefficient. This unphysical apparent behavior is due to the macroscopic diffusion potential that arises from the electrostatic interactions that are not accounted for in the Fick equation (Eq. (1)), but are accounted for in the electro-diffusion equation (Eq. (9)).

Also shown in Fig. 5 are the relative concentration differences for all the species present, as calculated by Eq. (9). For the $CaCl_2$/KI system, the "slow" species is the Ca^{2+} ion. For the K_2CO_3 system, it is the CO_3^{2-} ion. The effect of these two ions is to greatly control the macroscopic diffusion potential across the specimen. The relatively slow moving Ca^{2+} ions contribute to a diffusion potential in the $CaCl_2$ vessel that is positive with respect to the KI vessel. Correspondingly, the CO_3^{2-} ion contributes to a negative potential with respect to the KI vessel. The result is a macroscopic diffusion potential that attracts the iodide ion to the $CaCl_2$ vessel, and repels it from the K_2CO_3 vessel. In the $CaCl_2$/KI system, the macroscopic diffusion potential is sufficient to drive iodide from the KI vessel to the $CaCl_2$ vessel, even though the iodide concentration in the KI vessel is less than that of the $CaCl_2$ vessel. In time, the diffusion potential decreases and the concentration difference Δ approaches zero again.

8. Conclusions

The effect of speciation on the apparent diffusion coefficient of an ion can be dramatic in a nonreactive porous material. For the systems studied, the effect of concentration was to change the apparent diffusion coefficient by no more than 20%. By contrast, the effect of speciation on these nonreactive systems studied was to vary the apparent diffusion coefficient by nearly a factor of two at relatively short time. At long time the apparent diffusion coefficient became strongly time-dependent for some species. Such systems cannot be modeled using Fick's law and a constant apparent diffusion coefficient. Further, for one system studied, the apparent diffusion coefficient diverged to infinity, and then became *negative* for a period of time, due to the diffusion potential. The long time behavior of all the systems studied could be accurately characterized by an electro-diffusion equation containing only two time-independent parameters: the porosity and the formation factor.

Acknowledgments

The authors are indebted to Prof. Raymond Cook of the University of New Hampshire for performing a mercury intrusion porosimetry measurement on a ceramic frit specimen. KAS would also like to acknowledge the partial support of both the U.S. Nuclear Regulatory Commission and the Portland Cement Association.

References

[1] G. Achari, S. Chatterji, R.C. Joshi, Evidence of the concentration dependent ionic diffusivity through saturated porous media, in: L.-O. Nilsson, J.P. Ollivier (Eds.), Chloride Penetration Into Concrete, Rilem Publications, France, 1995, pp. 74–76.
[2] J. Arsenault, J.-P. Bigas, J.-P. Ollivier, Determination of chloride diffusion coefficient using two different steady-state methods: Influence of concentration gradient, in: L.-O. Nilsson, J.P. Ollivier (Eds.), Chloride Penetration Into Concrete, Rilem Publications, France, 1995, pp. 150–160.
[3] T. Zhang, O.E. Gjørv, Diffusion behavior of chloride ions in concrete, Cem. Concr. Res. 26 (1996) 907–917.
[4] L. Tang, Concentration dependence of diffusion and migration of chloride ions: Part 1. Theoretical considerations, Cem. Concr. Res. 29 (1999) 1463–1468.
[5] L. Tang, Concentration dependence of diffusion and migration of chloride ions: Part 2. Experimental evaluations, Cem. Concr. Res. 29 (1999) 1469–1474.
[6] H. Ushiyama, S. Goto, Diffusion of various ions in hardened Portland cement paste, The VI International Congress of the Chemistry of Cement, vol. II—Book 3, 1974 (Moscow).
[7] K.A. Snyder, The relationship between the formation factor and the diffusion coefficient of porous materials saturated with concentrated electrolytes: Theoretical and experimental considerations, Concr. Sci. Eng. (to be published December 2001).
[8] I. Rubinstein, Electro-Diffusion of Ions, SIAM, Philidelphia, 1990.
[9] L.-O. Nilsson, E. Poulsen, P. Sandberg, P. Sorensen, O. Klinghoffer, HETEK-Chloride Penetration Into Concrete, Report No. 53, The Road Directorate, Copenhagen, Denmark, 1996.
[10] K.A. Snyder, J.R. Clifton, J. Pommersheim, A computer program to facilitate performance assessment of underground low-level waste concrete vaults, in: W.M. Murphy, D.A. Knecht (Eds.), Scientific Basis for Nuclear Waste Management XIX, Mat. Res. Soc. Symp. Proc. 412, Materials Research Society, Pittsburgh, 1996, pp. 491–498.
[11] D.P. Bentz, J.R. Clifton, K.A. Snyder, Predicting service life of chloride-exposed steel-reinforced concrete, Concr. Int. 18 (1996) 42–47.
[12] E.J. Reardon, An ion interaction model for determination of chemical equilibria in cement/water systems, Cem. Concr. Res. 20 (1990) 175–192.
[13] J. Duchesne, E.J. Reardon, Measurement and prediction of portlandite solubility in alkali solutions, Cem. Concr. Res. 25 (1995) 1043–1053.
[14] R. Barbarulo, J. Marchand, K.A. Snyder, S. Prené, Dimensional analysis of ionic transport problems in hydrated cement systems: Part 1. Theoretical considerations, Cem. Concr. Res. 30 (2000) 1955–1960.
[15] J. Crank, The Mathematics of Diffusion, second ed., Oxford Univ. Press, New York, 1975.
[16] E.L. Cussler, Multicomponent Diffusion, Elsevier Scientific, 1976.
[17] M. Kato, Numerical analysis of the Nernst–Planck–Poisson system, J. Theor. Biol. 177 (1995) 299–304.
[18] A.E. James, J.D. Stillman, D.J.A. Williams, Finite element solution of the equations governing the flow of electrolyte in charged microporous membranes, Int. J. Numer. Methods Fluids 20 (1995) 1163–1178.

[19] E. Samson, J. Marchand, Numerical solution of the extended Nernst–Planck model, J. Coll. Interface Sci. 215 (1999) 1–8.
[20] E. Samson, J. Marchand, Modelling ion diffusion mechanisms in porous media, Int. J. Numer. Methods Engin. 46 (1999) 2043–2060.
[21] O. Truc, J.-P. Ollivier, L.-O. Nilsson, Numerical solution of multi-species diffusion, Mater. Struct. 33 (2000) 566–573.
[22] O. Truc, J.-P. Ollivier, L.-O. Nilsson, Numerical simulation of multi-species transport through saturated concrete during a migration test, Cem. Concr. Res. 30 (2000) 1581–1592.
[23] J. Bear, Dynamics of Fluids in Porous Media, Dover Publications, New York, 1988.
[24] F. Helfferich, Ion Exchange, McGraw-Hill, New York, 1962.
[25] C. Kittel, H. Kroemer, Thermal Physics, W.H. Freeman, San Francisco, 1980.
[26] J.O'M. Bockris, A.K.N. Reddy, Modern Electrochemistry, vols. 1–2, Plenum, Hingham, MA, 1970.
[27] E.A. Guggenheim, R.H. Stokes, Equilibrium Properties of Aqueous Solutions of Single Strong Electrolytes, Pergamon, 1969.
[28] K.S. Pitzer, Thermodynamics of electrolytes: I. Theoretical basis and general equations, J. Phys. Chem. 77 (1973) 268–277.
[29] L.N. Plummer, D.L. Parkhurst, G.W. Fleming, S.A. Dunkle, A computer program incorporating Pitzer's equations for calculation of geochemical reactions. In Brines, U.S. Geological Survey Report 88-4153, Reston, VA, 1988.
[30] R. Mills, V.M.M. Lobo, Self-Diffusion in Electrolyte Solutions, Elsevier, 1989.
[31] R.E. Collins, Flow of Fluids Through Porous Materials, Reinhold Publishing, 1961.
[32] D.L. Johnson, P.N. Sen, Dependence of the conductivity of a porous medium on electrolyte conductivity, Phys. Rev. B 37 (1988) 3502–3510.
[33] A. Revil, P.W.J. Glover, Theory of ionic-surface electrical conduction in porous media, Phys. Rev. B 55 (1997) 1757–1773.
[34] P.N. Sen, Unified model of conductivity and membrane potential of porous media, Phys. Rev. B 39 (1989) 9508–9517.
[35] A. Revil, Ionic diffusivity, electrical conductivity, membrane and thermoelectric potentials in colloids and granular porous media: A unified model, J. Colloid Interf. Sci. 212 (1999) 503–522.
[36] K.A. Snyder, C. Ferraris, N.S. Martys, E.J. Garboczi, Using impedance spectroscopy to assess the viability of the rapid chloride test for determining concrete conductivity, J. Res. NIST 105 (2000) 497–509.
[37] R.S. Barneyback, S. Diamond, Expression and analysis of pore fluid from hardened cement pastes and mortars, Cem. Concr. Res. 11 (1981) 279–285.
[38] R.E. McDuff, R.A. Ellis, Am. J. Sci. 279 (1979) 666–675.
[39] F.A. Settle (Ed.), Handbook of Instrumental Techniques for Analytical Chemistry, Prentice Hall, NJ, 1997.
[40] L.M. Schwartz, P.N. Sen, D.L. Johnson, Influence of rough surfaces on electrolytic conduction in porous media, Phys. Rev. B 40 (1989) 2450–2458.
[41] H.J.V. Tyrrell, K.R. Harris, Diffusion in Liquids, Butterworths, Ontario, Canada, 1984.
[42] B.N. Taylor, C.E. Kuyatt, Guidelines for Evaluating and Expressing the Uncertainty of NIST Measurement Results, National Institute of Standards and Technology, NIST Technical Note 1297, Gaithersburg, MD, 1993.